# Spatial Lesion Indexing for Medical Image Databases Using Force Histograms

Chi-Ren Shyu and Pascal Matsakis
{shyu, matsakis}@cecs.missouri.edu
Computer Engineering and Computer Science Department
University of Missouri-Columbia
Columbia, MO 65211-2060

**Abstract**

*It is often difficult to come up with a well-principled approach to the selection of a spatial indexing mechanism for medical image databases. Spatial information about lesions in medical images is critically important in disease diagnosis and plays an important role in image retrieval. Unfortunately, the images are rarely indexed properly for clinically useful retrieval. One example is the well-known R-tree and its variants which index image objects based on their physical locations in an "absolute" way. However, such information is not meaningful in medical content-based image retrieval systems, and the approaches above suffer from problems caused by variations in object size and shape, imprecise image centering, etc. A more appropriate approach, which does not require object registration, is to model the spatial relationships between the lesions and anatomical landmarks. To convey diagnostic information, lesions must exist in certain locations with regard to the landmarks. In this paper, we show that the histogram of forces (which represents the relative position between two objects) provides an efficient spatial indexing mechanism in the medical domain.*

**Keywords**: Spatial indexing, force histograms, medical image databases, content-based image retrieval.

## 1 Introduction

Examples now abound of medical content-based image retrieval systems (CBIR) that retrieve database images by characterizing textures of pathologies [23] [11], shapes of tumors [12], shapes of cardiac boundary curves [19] and symmetric properties of the brain ventrical line [4]. However, in addition to those isolated findings in medical images, physicians also look for the locations of lesions for supporting their diagnoses. More specifically, the related locations of lesions with respect to organ boundaries and to certain significant anatomical landmarks. Therefore, clinically meaningful spatial indexing on lesions is an urgent need for the existing medical CBIR systems.

To open our discussion on spatial indexing, a brief introduction on traditional database indexing is given in this section. Over the years, the following methods have become popular for the purpose of indexing in multi-dimensional feature spaces and for objects in two to three dimensional spaces: B-trees [5], R-trees [8], and their variants [2, 20, 21, 1]. These data structures fall into two groups: The first group contains tree structures created by partitioning the attributes on the basis of the values of image features such as texture, shape, gray-scale, etc. These tree structures include K-D-B tree [18], Metric tree [25] and Multi-hash indexing [23]. The common approach for these tree structures is to partition the attribute space into disjoint hyper-cubes, each containing a small number of pointers linking to a subset of images.

The second group also contains tree structures. Unlike the previous tree structures carving high-dimensional feature spaces, tree structures in this group partition the image space itself. In this type, a two- or three-dimensional image space is partitioned into several bounding rectangles or spheres to describe the locations of the extracted objects in the image. This approach includes R-tree [8], $R^+$-tree [21], $R^*$-tree [1], bounding spheres SS-tree [27], and bounding spheres and rectangles SR-tree [10]. Indexing methods in the second group were designed specifically for the purpose of localizing the extracted objects in an image. These methods are used when the locations of the extracted objects are invariate to scaling, translation, and rotation.

In addition to the traditional spatial indexing approaches, many CBIR researchers have made significant contributions for the modeling of spatial relationships for image retrieval. One of the promising examples is the SaFe system developed by Smith and Chang [24]. In this system, a 2-D string approach

[3] was applied to capture spatial relations, e.g., *adjacency, neareness, overlap*, and *surround*. However, the 2-D string approach is not enough when a retrieval engine requires numeric measurement beyond symbolic and logic spatial relationships.

From the standpoint of content-based image retrieval (CBIR), the challenge posed by medical images is that the lesions of the same diagnosis tend to be highly related to their spatial relationships with certain anatomic landmarks, often affecting the exact pixel location only minimally. For this reason, the traditional spatial indexing mechanism is no longer meaningful in medical CBIR systems. For example, in the domain of high resolution computed tomography (HRCT) lung images, a finding of two images with similar visual abnormalities is not enough to conclude that these two images bear the same disease, unless the following regional information can be confirmed: 1) central or peripheral, 2) upper or lower, 3) anterior or posterior, 4) unilateral or bilateral, and 5) the lobes where lesions are located [26].

The following questions remain: What is an appropriate spatial indexing mechanism in the medical domain? How to retrieve images with lesions bearing the same pathology and having similar spatial locations simultaneously? To answer the latter question, we have combined our recently developed CBIR engine for HRCT images of the lung with the spatial indexing mechanism. To answer the former question, we have applied the histogram of forces to model the spatial relationships between lesions and anatomical landmarks. Such a histogram represents the relative position between two objects [13] [14]. It is sensitive to their shape, orientation and distance. It has nice geometric properties, offers solid theoretical guarantees, and lends itself, with great flexibility, to the definition of fuzzy directional spatial relations (such as "to the right of", "to the south of", etc.) [15].

The paper is organized as follows. In Section 2, we describe the objects we are dealing with and we categorize the spatial relationships between these objects. Section 3 discusses the use of the histogram of forces to measure the spatial information. The measurements are the degrees of truth for spatial relationships among lesions and anatomical landmarks. In Section 4, a multi-dimensional indexing mechanism for fast image retrieval is presented. In addition, query methods are discussed which feature distance measurement from the spatial relationships among multiple lesions and chambers. Experimental results are then reported in Section 5 and the overall conclusion is in Section 6.

## 2 Objects and Relationships

Although our approach can be applied to different modalities of medical images, we focus here on HRCT images of the lungs. In our spatial model, there are two major object abstractions: *lesions* $L$ and *chambers* $C$. These objects can be obtained by human delineation, automatic region extraction algorithms, or contour extraction algorithms (*e.g.*, [23]). In this paper, we assume these objects are successfully extracted and ready for spatial indexing.

A *lesion* is a pathological region identified by a physician. A *chamber* is part of a lung. It is defined by anatomical landmarks, such as the lung boundary and the fissures that are present in each lung. The left lung has one fissure, "left-oblique" (LO), and the right lung has two that are "right-horizontal" (RH) and "right-oblique" (RO). The fissures divide each of the lungs into chambers. The left side of an HRCT lung image would ideally show two fissures and the right side one because the right lung has three chambers and the left lung two. Only a subset of these fissures is visible in most images in our database. Fissure may or may not be visible depending on where exactly a lung cross-section is taken. In Fig. 1(a), there is only one fissure RH that divides right lung into two chambers. Each of these chambers thus generated carries a unique label as shown in Table 1. The fourth column of this table lists the number of cases archived in our current database.

As mentioned before, the location of pathology plays an important role in disease diagnosis, and, as a consequence, also plays an important role in image retrieval. The pathology bearing pixels must exist in certain locations with regard to a chosen set of anatomical landmarks in order to convey diagnostic information. For example, both centrilobular emphysema (CLE) and paraseptal emphysema (PSE) show low-attenuation areas in HRCT images. However, CLE is always interior to a chamber and PSE is always adjacent to either the lung boundary or one of the fissures. The spatial relations between lesions (L) and chambers (C) can be categorized by the following operators (*op*):

1. $L$ *op* $L \rightarrow$ direction (left, right, above, below)
2. $L$ *op* $L \rightarrow$ touch (meet, apart)
3. $L$ *op* $C \rightarrow$ areas (intersection)
4. $L$ *op* $C \rightarrow$ direction (left, right, above, below)
5. $L$ *op* $C \rightarrow$ adjacency (adjacent, interior, cover)

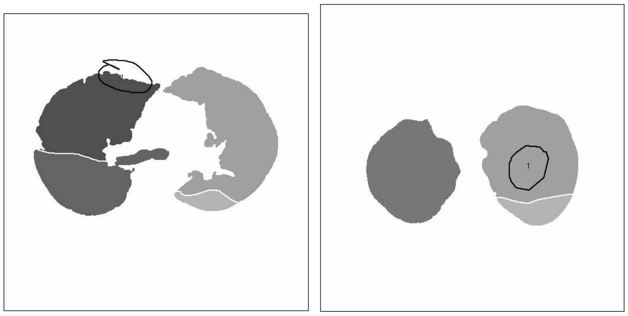

(a) (b)

Figure 1: *(a) Two chambers, $C^H_{RU}$ and $C^H_{RL}$ appear in the right lung and two chambers, $C^O_{LU}$ and $C^O_{LL}$ in the left lung. A lesion is marked adjacent to $C^H_{RU}$. (b) Only one chamber $C^\phi_R$ in right lung and two chambers, $C^O_{LU}$ and $C^O_{LL}$ in the left lung. A lesion is marked interior to $C^O_{LU}$.*

Table 1: *Chambers of lungs.*

| Chambers | Landmarks | label | No. of cases |
|---|---|---|---|
| left | $\phi$ | $C^\phi_L$ | 457 |
| left upper | Oblique | $C^O_{LU}$ | 2690 |
| left lower | Oblique | $C^O_{LL}$ | 2690 |
| right lung | $\phi$ | $C^\phi_R$ | 636 |
| right upper | Horizontal | $C^H_{RU}$ | 1781 |
| right upper | Oblique | $C^O_{RU}$ | 2311 |
| right middle | Both | $C^B_{RM}$ | 124 |
| right lower | Horizontal | $C^H_{RL}$ | 2380 |
| right lower | Oblique | $C^O_{RL}$ | 1132 |

## 3 Measuring Spatial Information

### 3.1 The Histogram of Forces

Knowing how to apprehend the spatial organization of 2-D objects is essential to computer vision (for pattern recognition, image understanding, scene description in natural language, etc.). Freeman [6] proposed that the relative position of objects be described in terms of primitive spatial relations (e.g., "below", "near", and "surround"). He also proposed that fuzzy relations be used. By introducing the notion of the histogram of angles, Miyajima and Ralescu [17] developed the idea that the relative position between two objects can have a representation of its own and can thus be described in terms other than spatial relations. In [13] [14], Matsakis and Wendling introduced the notion of the histogram of forces, which generalizes and supersedes that of the histogram of angles. The relative position of a 2D object $A$ with regard to another object $B$ is represented by a function $F^{AB}$ from $\Re$ into $\Re^+$. For any direction $\Theta$, the value $F^{AB}(\Theta)$ is the scalar resultant of elementary forces. These forces are exerted by the points of $A$ on those of $B$, and each tends to move $B$ in direction $\Theta$ (Fig. 2). $F^{AB}$ is called *the histogram of forces* associated with ($A$,$B$) *via* F, or the *F-histogram* associated with ($A$,$B$). The object $A$ is the *argument*, and the object $B$ the *referent*. $F^{AB}$ encapsulates a large amount of information about $A$ and $B$. It is sensitive to their shape, orientation and distance. Moreover, it has nice geometric properties: when a translation is applied to A and B, the histogram does not change; when a rotation is applied, the histogram is simply shifted along the x-axis; when a dilation is applied, the histogram is stretched. After applying some translations and/or dilations to A and B, the normalized F-histogram associated with the transformed objects A' and B' is equal to the normalized F-histogram associated with A and B. This is natural, since the relative position between A' and B' and the relative position between A and B are obviously the same. The inverse problem is complex and remains to be solved. However, if the F-histograms associated with two pairs of objects are the same, the two pairs are most likely the same (up to a translation and/or a dilation).

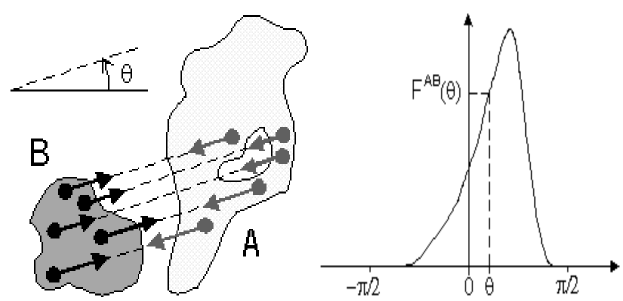


Figure 2: *Computation of $F^{AB}(\Theta)$.*

In practice, of course, a histogram is represented by a limited number of values. Each value is the scalar resultant of forces exerted in some direction. Its computation translates into the assessment of predetermined algebraic expressions. In the case of raster data, each assessment corresponds to the process of a pair of segments (more precisely, a batch of pairs of pixels). The generation of these segments is based on the rasterization of a group of parallel lines by means of Bresenham's algorithm in integer arithmetic. The maximum complexity of F-histogram computation is $O(kn\sqrt{n})$, where $n$ denotes the number of pixels of the processed image and $k$ the number of directions in which forces are computed. This complexity drops to $O(kn)$ for convex objects. Note that F-histogram computation is highly parallelizable, and that Bresenham's algorithm is commonly circuit coded in visualization systems.

### 3.2 Computing Degrees of Truth

The histogram of forces is a powerful tool of representation. It lends itself, with great flexibility, to the definition of directional spatial relations (such as "to the right of", "above", etc.). Let $A$ and $B$ be two objects, *i.e.*, lesions, chambers or lungs. As shown in [15], the degree of truth of the proposition "$A$ is in direction $\Theta$ of $B$ " can be extracted from the analysis of $F^{AB}$, for any angle $\Theta$. The degree of truth is a real number greater than or equal to 0 (proposition completely false) and less than or equal to 1 (proposition completely true).

We now introduce a model of "inner-adjacency", which is another clinically meaningful spatial relationship. We consider histograms of constant forces (the elementary force exerted by one point on another is independent of the distance between these points [13][14]). We represent each one by 64 bins (with smaller bins, comparable results would be achieved, and the computation time would get higher). As a matter of fact, in this paper, we describe the position of $A$ relative to $B$ by the force histogram associated with ($A$,$B$-$A$), and not by $F^{AB}$. Some histogram values may thus be null even when $A$ and $B$ intersect. This property allows us to model "inner-adjacency" as follows: the degree of truth of the proposition "$A$ is inner-adjacent to $B$" is set to $max(\frac{i}{b}, min(\frac{i}{a}, 1 - \frac{h_{min}}{h_{mean}}))$, where $a$ denotes the size of $A$ and $b$ the size of $B$ (in pixels), $i$ is the intersection of $A$ and $B$, and $h_{min}$ and $h_{mean}$ are the minimum and average values of the histogram. Figure 3 shows 8 configurations and the degrees of truth obtained for the two propositions "$A$ is inner-adjacent to $B$" and "$A$ is to the right of $B$" (*i.e.*, "$A$ is in direction 0 of $B$"). Note that the degrees of truth of "$A$ is above $B$" (*i.e.*, "$A$ is in direction 90 degrees of $B$"), "$A$ is to the left of $B$", and "$A$ is below $B$" are all null.

Table 2: *Elements in spatial vector.*

| number | description | data type and domain |
|---|---|---|
| 1 | Chamber label | labels from Table 1 |
| 2 | $0^o$ degree of truth | [0.0,1.0] |
| 3 | $90^o$ degree of truth | [0.0,1.0] |
| 4 | $180^o$ degree of truth | [0.0,1.0] |
| 5 | $270^o$ degree of truth | [0.0,1.0] |
| 6 | Principal direction | [0,360] |
| 7 | Intersection | [1, size(lesion)] |
| 8 | Interior_Adjacent | [0.0,1.0] |

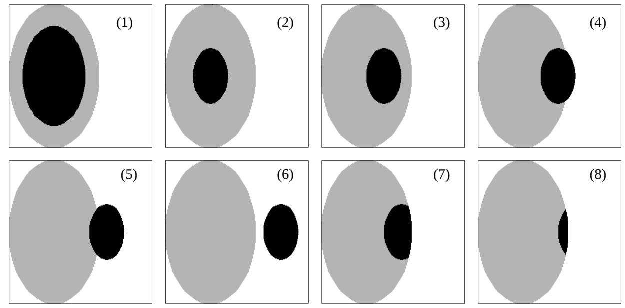


Figure 3: *The degree of truth for (Inner-Adjacent, To_The_Right): (1) (0.34,0.00) (2) (0.15,0.00) (3) (0.55,0.31) (4) (0.83,0.84) (5) (0.21,0.99) (6) (0.00,1.00) (7) (1.00,0.82) (8) (1.00,0.96)*

## 4 Spatial Indexing and Retrieval

Each lesion $L_{I_{DB}}$ in a database image $I_{DB}$ is represented by one or more eight dimensional spatial vectors $f^{L_{I_{DB}}}$. For lesions shown in Fig. 1, only one feature vector is needed to represent each lesion from both cases since each of them resides in only one chamber. For lesions present in multiple chambers, multiple feature vectors will be formed. Table 2 lists the description and data types for those eight elements in $f^{L_{I_{DB}}}$.

For each database image, we compute the above measurements for each lesion-chamber pair in the image. We then build a metric tree [25] for fast retrieval. This tree structure has been proven efficient for nearest neighbor search in the context of CBIR [9]. Two types of spatial queries are provided in our approach: single-lesion retrieval and multiple-lesion retrieval.

Let $L_{q_i}$ be the $i$-th lesion in a query image $I_q$, $1 \leq i \leq |L_q|$, and $L^{n_j}$ be the $j$-th lesion in the $n$-th database image $I_D^n$, $1 \leq j \leq |L_n|$. For a single lesion query, $|L_q| = 1$, the spatial features are computed between the lesion and all intersecting chambers. A three dimensional feature vector is then formed and parsed to the metric tree. $N$ nearest neighbors are thus retrieved from the database. Fig 4 shows a query lesion and its retrieval results.

To query multiple lesions, the system first retrieves and ranks database lesions based on the similarities of their spatial features to the query lesion(s) individually. Let $S_i$ be the set of retrieved database lesions for query lesion $L_{q_i}$ and $I_{dbs}^i$ be the set of database images that have lesions $S_i$. Assuming we would like to retrieve $N$ best matching images. Ideally, retrieval results can be obtained by $\cap_{k=1}^{|L_q|} I_{dbs}^k$. However, if there is an insufficient number of images returned from the conjunction set, the system could either increase $N$ or

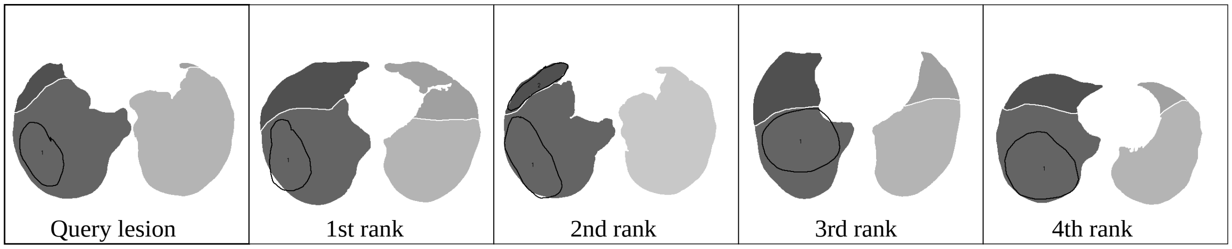


Figure 4: *A single query lesion and its four best matching lesions.*

relax the query by removing a set of lesions $S_r$ from the query.

## 5 Experimental Evaluation

In order to demonstrate the usefulness of our approach in the medical domain, we have collected $2,080$ HRCT images of lungs with $3,980$ lesions as our testbed. One expert physician and three non-expert users were asked to evaluate the retrieval results. A list of guidelines and evaluation items is provided to the users. The guidelines include: 1. A tutorial of important spatial relationships in HRCT lung images. 2. Image examples from different lesion spatial relationships. 3. Examples from good retrieval results and also bad retrieval results. The evaluation items are: 1. Correctness of chambers where the best matching lesions are present. 2. Correctness of interior or adjacent spatial relationships between lesions and chambers from the retrieval results. 3. Correctness of principal directions from the results, such as to_the_right, to_the_top, to_the_bottom, and to_the_left. Each evaluation item has a scale from 0 to 10. A perfect retrieval result should get a 10. We conducted this evaluation by randomly selecting 20 query cases from the database and retrieving the best 10 cases to the users. Database images from the query patient's images were not retrieved. The users were asked to evaluate each retrieval result by assigning a score to each evaluation item. Table 3 lists evaluations done by the users. A full score from theses 200 retrieval results is 2000. From the evaluations, the physician agrees with 90% of the retrieval results with correct interior or adjacent spatial relationships and 81% for the lesion's principal direction with respect to the chambers. The evaluations from three non-expert users vary. On average, they agree with 89% of retrieval results in the relationship of interior or adjacent and 76% in principal direction. Part of the reason for these unsatisfactory results are unsuccessful chamber extractions or lesion extractions. For a clinically useful spatial relationship, such as interior or adjacent, our approach achieves a 90% accuracy rate.

Table 3: *User's evaluations.*

| User's class | Chamber | Int or Adj | Direction |
|---|---|---|---|
| Physician | 1921/2000 | 1805/2000 | 1624/2000 |
| Non-expert 1 | 1887/2000 | 1760/2000 | 1328/2000 |
| Non-expert 2 | 1802/2000 | 1723/2000 | 1566/2000 |
| Non-expert 3 | 1780/2000 | 1878/2000 | 1691/2000 |

## 6 Discussion and Conclusion

We presented a new lesion spatial indexing mechanism for lung HRCT image databases. Compared to current existing spatial indexing methods, our approach is robust and able to achieve high accuracy rates for spatial lesion retrieval. We intend to extend our approach to different medical image modalities, such as brain MR images. Other interesting future directions include: 1. studying of other features that are also meaningful in medical domain, 2. modeling spatial relationship between lesions, 3. standardizing evaluation methods for retrieval results, and 4. integrating this work with medical CBIR systems that retrieve images with similar pathologies.

## References

[1] Beckmann et al., The $R^*$-tree: An efficient and robust access method for points and rectangles, in *Proc. of ACM SIGMOD*, pp. 322-331, 1990.

[2] J. L. Bentley and J. H. Friedman, Data structures for range searching, *ACM Computing Surveys*, 11(4):397-409, December 1979.

[3] S.-K. Chang, Q. Y. Shi, and C. Y. Yan, Iconic indexing by 2-D strings, *IEEE Transactions on Pattern Anal. and Machine Intell.*, Vol. 9, No. 3, pp. 413-428, 1987.

[4] W. W. Chu, C. C. Hsu, A. F. Cardenas and R. K. Taira, A knowledge-based image retrieval with spatial and temporal constructs, *IEEE Transactions on Knowledge and Data Engineering*, Vol. 10, No. 6, pp. 872-888, 1998.

[5] D. Comer, The ubiquitous B-Tree, *ACM Computing Surveys* 11,2, June 1979.

[6] J. Freeman, The modeling of spatial relations, *Computer Graphics and Image Processing*, Vol. 4, pp. 156-171, 1975.

[7] R. H. Guting, An introduction to spatial database systems, *VLDB Journal*, 3, pp. 357-399, 1994.

[8] A. Guttman, R-Trees: A dynamic index structure for spatial searching, in *Proc. of ACM SIGMOD*, pp. 47-57, June 1984.

[9] J. Harnsomburana, A hybrid tree approach for fast image database retrieval with dynamic feedback, *MS Thesis, CECS Department, University of Missouri-Columbia*, December 2001.

[10] T. Kato, T. Kurita, and H. Shimogaki, Intelligent visual interaction with image database systems - toward the multimedia personal interface- *Journal of Information Processing*, Vol. 14, No. 2, pp.134-143, 1991.

[11] P.M. Kelly, T.M. Cannon, and D.R. Hush, Query by image example: The CANDID approach, in *SPIE Vol. 2420 Storage and Retrieval for Image and Video Databases III*, pp. 238-248, 1995.

[12] F. Korn, N. Sidiropoulos, C. Faloutsos, E. Siegel, Z. Protopapas, Fast and effective retrieval of medical tumor shapes, *IEEE Transactions on Knowledge and Data Engineering*, Vol. 10, No. 6, pp. 889-904, 1998.

[13] P. Matsakis, *Relations spatiales structurelles et interpretation d'images*, Ph. D. Dissertation, Institut de Recherche en Informatique de Toulouse, France, 1998.

[14] P. Matsakis, L. Wendling, A new way to represent the relative position of areal objects, *IEEE Pattern Analysis and Machine Intelligence*, vol. 21, no. 7, pp. 634-643, 1999.

[15] P. Matsakis, J. Keller, L. Wendling, J. Marjamaa, O. Sjahputera, Linguistic description of relative positions in images, *IEEE Trans. on Systems, Man and Cybernetics, Part B*, Vol. 31, No. 5, pp. 573-588, 2001.

[16] F. H. Netter, *Atlas of Human Anatomy*, CIBA-GEIGY Limited, Basle Switerland, 1989.

[17] K. Miyajima, A. Ralescu, Spatial organization in 2D segmented images: representation and recognition of primitive spatial relations, *Fuzzy Sets and Systems*, Vol. 65, Iss. 2/3, pp. 225-236, 1994.

[18] J. T. Robinson, The k-d-b tree: A search structure for large multi-dimensional dynamic indexes, in *Proc. of ACM SIGMOD*, pp. 10-18, 1981.

[19] G. P. Robinson, H. D. Tagare, J. S. Duncan, and C. C. Jaffe, Medical image collection indexing: shape-based retrieval using KD-tree, *Computerized Medical Imaging and Graphics*, Vol. 20, No. 4, pp. 209-217, 1996.

[20] N. Roussopoulos and D. Leifker, Direct spatial search on pictorial databases using packed R-trees, *Proc. ACM SIGMOD*, May 1985.

[21] T. Sellis, N. Roussopoulos, and C. Faloutsos, The $R^+$-tree: A dynamic index for multidimensional objects, *Proc. of 13th Internal Conference on VLDB*, pp. 507-518, England, September 1987.

[22] C. R. Shyu, A. C. Kak, C. E. Brodley, and L. S. Broderick, Testing for human perceptual categories in a physician-in-the-loop CBIR system for medical imagery, to appear in *Proc. IEEE Workshop of Content-Based Access of Image and Video Databases*, Fort Collins, CO, June 1999.

[23] C. R. Shyu, C. E. Brodley, A. C. Kak, A. Kosaka, A. M. Aisen and L. S. Broderick, ASSERT: A physician-in-the-loop content-based image retrieval system for HRCT image databases, *Computer Vision and Image Understanding*, Vol. 75, Nos. 1/2, July/August, pp. 111-132, 1999.

[24] J. R. Smith, Integrated Spatial and Feature Image Systems: Retrieval, Analysis and Compression , *Ph.D. Thesis, Columbia University, 1997.*

[25] J. K. Uhlmann, Satisfying general proximity/ similarity queries with metric trees, *Information Processing Letters*, 40(1991), pp. 175-179.

[26] W. R. Webb, N. L. Muller, and D. P. Naidich, *High-Resolution CT of The Lung*, second edition, Lippincott-Raven, Philadelphia, 1996.

[27] D. A. White and R. Jain, Similarity indexing with the ss-tree, *Proc. 12th Intl. Conf. on Data Engineering*, pp. 516-523, 1996.